8th International Symposium on Magnetic Bearing
August 26-28, 2002, Mito, Japan

NON-CONTACT LEVITATION CONTROL SYSTEM FOR ELECTROSTATIC MOTOR

Hidehiko Yasui
Akio Yamamoto
Toshiro Higuchi
Dept. of Precision Eng., The University of Tokyo, Bunkyo, Tokyo, 113-8656 Japan
{hide, akio, higuchi}@intellect.pe.u-tokyo.ac.jp

ABSTRACT

Non-contact levitation control systems for electrostatic motor are reported in this paper. The authors have developed high-power electrostatic linear motor called *Dual Excitation Multiphase Electrostatic Drive* (DEMED). DEMED is a linear synchronous motor and consists of pairs of thin plates and possesses a power per weight ratio of 230W/kg and acceleration of over 100G in open loop systems in dielectric liquid. These performances are higher than those of typical electromagnetic drives.

In this paper, non-contact levitation control systems for DEMED are proposed. A levitated motor using DEMED utilizes the same electrodes for thrust force generation and slider levitation. For controlling attractive force, bias voltage is superposed onto driving voltages.

INTRODUCTION

The authors have developed high-power electrostatic linear motor [1]. The electrostatic motor called *Dual Excitation Multiphase Electrostatic Drive* (DEMED) is direct-drive linear motor, and is compact in structure. DEMED can demonstrate high-efficiency, high-controllability, and high-power performances such as 230W/kg of power per weight ratio and 1.4m/s of maximum operation speed [2-3].

From the following points of view, DEMED seems to be suitable for a direct drive linear actuator in vacuum environment. In some vacuum applications using electron beam such as EB lithography and SEM, existence of electro-magnetic field is a fatal problem. Therefore, electromagnetic motors are less likely to be used for such applications. On the other hand, electrostatic motors generate less magnetic field, because they are driven with higher voltage and correspondingly lower current. Furthermore, DEMED excels at saving space in vacuum chamber, because of its compact structure.

It is well known that friction force becomes larger in vacuum environment. Therefore, it is desired that motors used in vacuum environment do not have mechanical contact parts. To adapt DEMED to vacuum environment, development of improved system having no mechanical contact parts are needed. Non-contact levitation of electrostatic motor can meet the need.

In past researches, some electrostatically levitated actuators are reported [4-6]. Those levitated actuator employs different electrodes for thrust force generation and levitation. In this paper, we propose non-contact levitation systems for DEMED, which utilize the same electrodes for thrust force generation and levitation. Firstly, gap-dependence of DEMED characteristics is investigated. Secondly, using bias voltage for controlling attractive force is proposed. Finally, three types of control systems of electrostatic levitated motor are proposed and discussed.

DUAL EXCITATION MULTIPHASE ELECTROSTATIC DRIVE (DEMED) [1]

In this section, conventional DEMED, which slider is not levitated, is introduced. A basic structure of DEMED is shown in Figure 1. DEMED consists of a pair of flat films, slider and stator, respectively. Both films are made of polyimide and contain copper electrodes. The electrodes are aligned with a constant pitch. Electrodes on slider and stator are connected into three phases, respectively. The electrode pitch is the same both in stator and in slider. The shape of electrodes is straight in stator, and washboard-shaped in

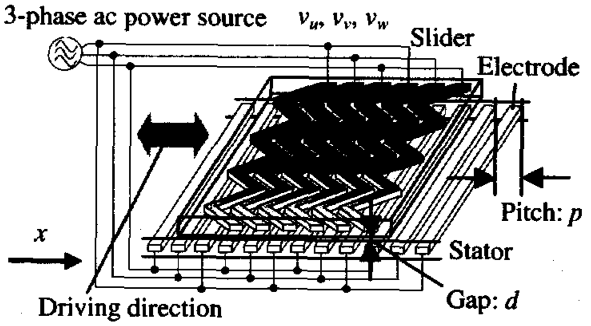

FIGURE 1: Dual Excitation Multiphase Electrostatic Drive

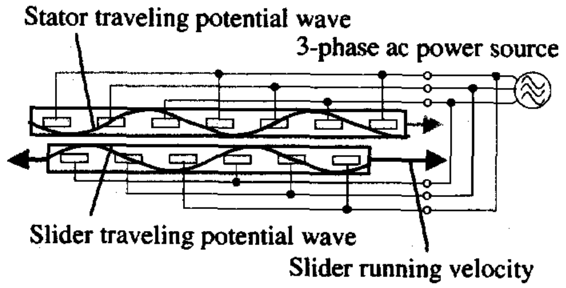

FIGURE 2: Driving principle

slider. Adapting the washboard-shaped electrodes can reduce force ripples of DEMED considerably [7]. Slider is just placed on stator without any mechanical guide. (In the levitated systems proposed later, slider is suspended beneath stator.) A gap between the slider and the stator is maintained around 20μm by glass beads inserted between slider and stator.

For driving, three-phase ac voltage is applied to the both three poles of stator and slider. The connections of three-phase ac voltages are opposite on slider and on stator. Applying ac voltage causes traveling potential waves on stator and slider as shown in Figure 2. The electrostatic interaction between two potential waves gives thrust force to the slider.

Performance of DEMED is closely related to capacitance coefficients among six poles of the electrodes. The relationship among six poles can be modeled as six-terminal network. The six-terminal network model of DEMED is shown in Figure 3. The relationships between the terminals are expressed by capacitors. In this model, resistances representing dielectric loss are ignored to simplify discussions. This network can be expressed by 6x6 matrix C. This matrix is called capacitance coefficients matrix, and correlate electric charges with voltage on each pole as:

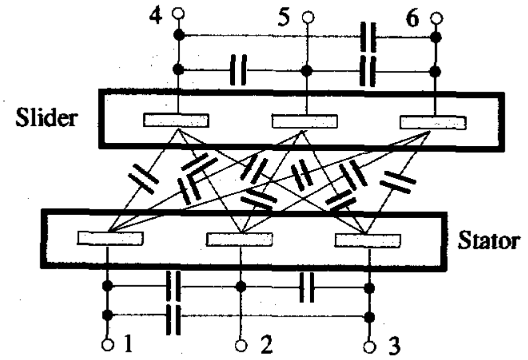

FIGURE 3: Electric circuit model of DEMED

$$q = Cv \tag{1}$$

where q is 6x1 column vector, expressing electric charges on each pole, and v is 6x1 column vector expressing voltage on each pole.

DEMED's thrust force f_x can be calculated as:

$$f_x = \frac{1}{2} v^t \frac{\partial C}{\partial x} v \tag{2}$$

where x is a displacement of slider against stator in thrust force direction.

The capacitance coefficients matrix C is a function of both slider displacement x and gap d between slider and stator. In our past research, we have proposed approximation of matrix C under the condition where gap d is constant, by considering symmetry among six poles [8]. The approximation of matrix C is a symmetric matrix and is given as:

$$C(x)_{d=const.} = \begin{bmatrix} C_{st} & C_t & C_t & C_m(x) & C_m(x+p) & C_m(x-p) \\ C_t & C_{st} & C_t & C_m(x-p) & C_m(x) & C_m(x+p) \\ C_t & C_t & C_{st} & C_m(x+p) & C_m(x-p) & C_m(x) \\ C_m(x) & C_m(x-p) & C_m(x+p) & C_{sl} & C_l & C_l \\ C_m(x+p) & C_m(x) & C_m(x-p) & C_l & C_{sl} & C_l \\ C_m(x-p) & C_m(x+p) & C_m(x) & C_l & C_l & C_{sl} \end{bmatrix} \tag{3}$$

where C_{st}, C_{sl}, C_t, C_l are constants. The element $C_m(x)$ represents capacitance coefficient between slider electrode and stator electrode, and is defined as:

$$C_m(x) = -C_0 - C_a \cos(\frac{2\pi}{3p} x) \tag{4}$$

where C_0 and C_a are constants. When voltage vector v is given as [v_0 sin(ϕ), v_0 sin(ϕ-2π/3), v_0 sin(ϕ+2π/3), v_0

$\sin(\phi)$, $v_0 \sin(\phi+2\pi/3)$, $v_0 \sin(\phi-2\pi/3)$], thrust force f_x can be calculated from equation (2) and (3) as follows:

$$f_x = \frac{3\pi C_a}{2p} v_0^2 \sin(2\phi + \frac{2\pi}{3p}x + \frac{\pi}{3}) \qquad (5)$$

where p represents electrode pitch. This thrust force characteristics is too complex for servo control of DEMED, therefore, we introduced the following control principle to simplify the characteristics. In the control principle, the phase ϕ of driving voltage is kept in accordance to slider displacement x to satisfy the following equation:

$$2\phi + \frac{2\pi}{3p}x + \frac{\pi}{3} = \frac{\pi}{2} \qquad (6)$$

Then, thrust force f_x is rewritten as equation (7) and can be easily controlled by using amplitude of driving voltage v_0.

$$f_x = \frac{3\pi C_a}{2p} v_0^2 \qquad (7)$$

RELATIONSHIP BETWEEN DEMED'S PERFORMANCE AND GAP

In this section, we discuss the DEMED's performance associated with gap d. Characteristics of attractive force between slider and stator is discussed, as well as those of thrust force.

Capacitance Coefficients Measurement

In our past research, DEMED have been evaluated at a certain value of gap d. However, capacitance coefficients of DEMED depend on gap d as well as x. In this study, we investigated variations of capacitance coefficients, thrust force, and attractive force with respect to d.

DEMED's attractive force f_d can be calculated from the following equation:

$$f_d = \frac{1}{2} v' \frac{\partial C(x,d)}{\partial d} v \qquad (8)$$

matrix $C(x, d)$, C_{st}, C_{sl}, C_t, and C_l in equation (4) becomes functions of gap d. Element C_m becomes a function of x and d, and is expressed as follows.

$$C_m(x,d) = -C_0(d) - C_a(d)\cos(\frac{2\pi}{3p}x) \qquad (9)$$

From equation (8) and (9), thrust force and attractive force is calculated as follows.

$$\begin{cases} f_x = \dfrac{3\pi C_a(d)}{2p} v_0^2 \sin(2\phi + \dfrac{2\pi}{3p} + \dfrac{\pi}{3}) \\ f_d = \dfrac{3}{4}\left\{k_0(d) - 3\dfrac{\partial C_a(d)}{\partial d}\cos(2\phi + \dfrac{2\pi}{3p} + \dfrac{\pi}{3})\right\} v_0^2 \end{cases} \qquad (10)$$

where $k_0(d)$ is

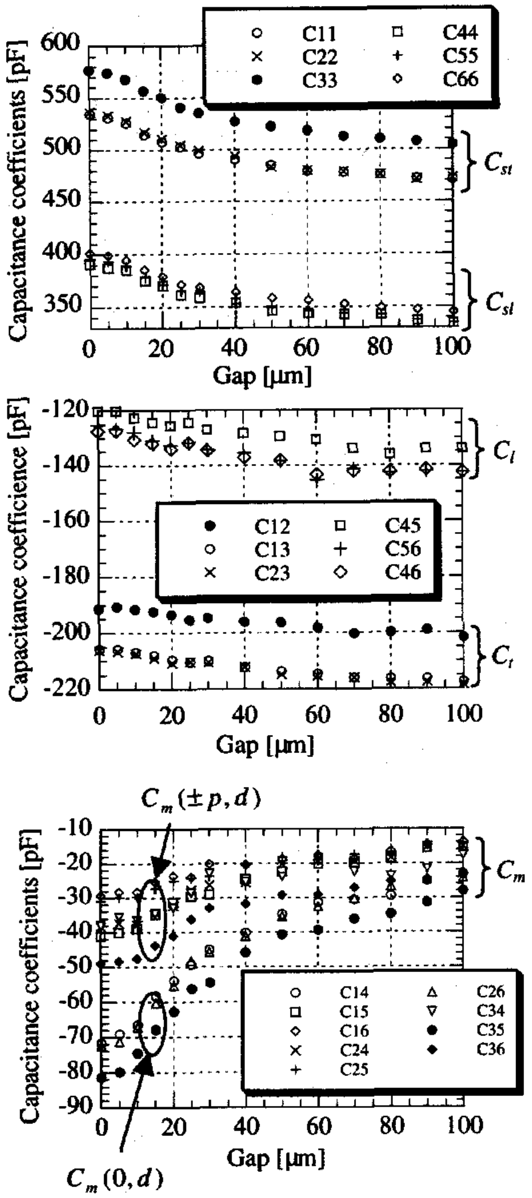

FIGURE 4: Measured capacitance coefficients

$$k_0(d) = \frac{\partial}{\partial d}(C_{st}(d) + C_{sl}(d) - C_t(d) - C_l(d) - 3C_0(d)) \qquad (11)$$

When f_x is controlled to satisfy equation (6), these forces are rewritten as:

$$\begin{cases} f_x = \dfrac{3\pi C_a(d)}{2p} v_0^2 \\ f_d = \dfrac{3}{4} k_0(d) v_0^2 \end{cases} \qquad (12)$$

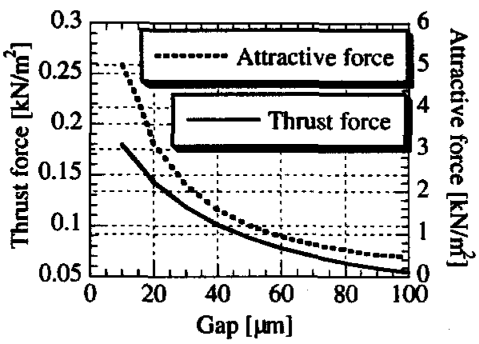

FIGURE 5: Relationship between gap and forces calculated from capacitance coefficients

We measured relationships between gap d and elements of $C(x,d)$ at $x = 0$. Results are shown in as shown in Figure 4. DEMED used in the measurement has electrode pitch of 200μm and effective electrode area of 16cm^2. According to the approximated model shown as equation (3), C_{11}, C_{22}, and C_{33} (= C_{st}) should be the same. However, electrodes in the real DEMED are not perfectly symmetry. Resultantly, measured elements are not completely the same. Same applies to C_{44}, C_{55}, and C_{66}. Measured data of C_{14}, C_{26}, and C_{35} expresses

$$C_m(0,d) = -C_0(d) - C_a(d) \tag{13}$$

Similarly, C_{15}, C_{16}, C_{24}, C_{25}, C_{34}, and C_{36}, expresses

$$C_m(\pm p,d) = -C_0(d) + \frac{1}{2}C_a(d) \tag{14}$$

Figure 4 shows that capacitance coefficients of DEMED are inversely proportional to gap d in the range of gap over 20μm. Functions C_{st}, C_{sl}, C_t, and C_l are approximated by averaging associating measured data as:

$$\begin{cases} C_{st}(d) = \dfrac{2.72\times10^{-3}}{d+2.82\times10^{-5}} + 467 \\ C_{sl}(d) = \dfrac{2.24\times10^{-3}}{d+2.82\times10^{-5}} + 321 \quad \text{[pF]} \\ C_t(d) = -\dfrac{0.593\times10^{-3}}{d+2.82\times10^{-5}} - 217 \\ C_l(d) = -\dfrac{0.997\times10^{-3}}{d+2.82\times10^{-5}} - 148 \end{cases} \tag{15}$$

Similarly, from equation (13) and (14), C_0 and C_a are approximated as:

$$\begin{cases} C_0(d) = -\dfrac{3.03\times10^{-3}}{d+2.82\times10^{-5}} \quad \text{[pF]} \\ C_a(d) = -\dfrac{0.467\times10^{-3}}{d+2.82\times10^{-5}} \end{cases} \tag{16}$$

Force Calculation

From equation (7), (12), (15), and (16), thrust force and attractive force at $v_0 = 1\mathrm{kV_{0\text{-}p}}$ are calculated as functions of gap d, as shown in Figure 5. Two curves in Figure 5 show that thrust force is inversely proportional to gap d and that attractive force is inversely proportional to square of d, as we can calculate from equations (11), (15), and (16).

LEVITATION CONTROL SYSTEM

In this section, levitation control system is discussed for controlling both of thrust force and attractive force independently. Equation (12) states that thrust force f_x and attractive force f_d are always proportional to each other. Therefore, thrust force f_x and attractive force f_d cannot be controlled independently. To realize levitated motor, we must control f_d independently from f_x. For that purpose we propose to apply bias voltage to stator electrodes.

In DEMED, three-phase driving voltages v_0 are supplied to slider and stator. We propose to superpose variable bias voltage v_b to the voltages of stator (or slider) electrode. Superposing bias voltage makes voltage vector $\boldsymbol{v}$ [$v_0\sin(\phi)$, $v_0\sin(\phi\text{-}2\pi/3)$, $v_0\sin(\phi+2\pi/3)$, $v_0\sin(\phi)+v_b$, $v_0\sin(\phi+2\pi/3)+v_b$, $v_0\sin(\phi\text{-}2\pi/3)+v_b$]. From equation (2) and (8), thrust force and attractive force are calculated as follows:

$$\begin{cases} f_x = \dfrac{3\pi C_a(d)}{2p} v_0^2 \\ f_d = \dfrac{3}{4}\left(k_0(d)v_0^2 + k_b(d)v_b^2\right) \end{cases} \tag{17}$$

where, $k_b(d)$ is:

$$k_b(d) = \frac{\partial}{\partial d}\left(2C_{sl}(d) - 4C_l(d)\right) \tag{18}$$

Equation (17) indicates that bias voltage does not affect thrust force. Therefore using bias voltage gives us some possibility to control f_x and f_d independently

To verify the theoretical consideration stated above, effect of bias voltage is investigated experimentally. For the force measurement, universal force-moment sensor system (UFS-20A05, NITTA co.) is utilized. Driving voltage and bias voltage are amplified by high voltage amplifier (Model 609C, TREK, INC.). For the measurement, DEMED which electrode pitch is 500μm was utilized. Statically measured thrust force and attractive force are shown in Figure 6. Figure 6 (a) indicates that attractive force increases in accordance with bias voltage independently of driving voltage. Figure 6 (b) indicates that bias voltage does not affect thrust force, as theory predicted.

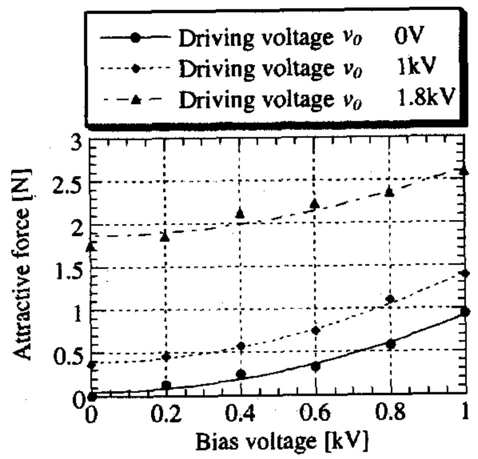

(a) Attractive force vs. bias voltage when driving voltage is 0V, 1kV, and 1.8kV

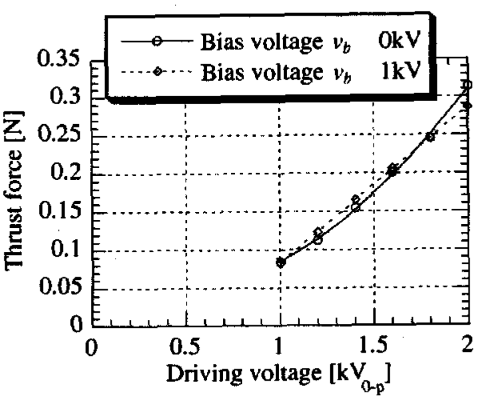

(b) Thrust force vs. driving voltage when bias voltage is 0V and $1kV_{0-p}$

FIGURE 6: Effect of bias voltage on thrust force and attractive force

In the following sections, three types of concrete levitation systems using bias voltage are proposed with schematic diagram. In the following systems, slider is suspended electrostatically just beneath the stator.

Type 1

Figure 7 shows a schematic view of Type 1 levitated motor. Thrust force and attractive force of this type are given by equation (17). In this type, thrust force f_x is controlled using v_0. To realize levitation, f_d must be controlled to stabilize the gap d. In steady state, f_d becomes almost equal to slider weight. Although changing v_0 for thrust force control affects attractive force, we can compensate the affect by using v_b. In

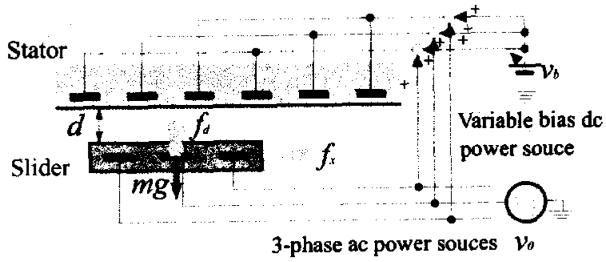

FIGURE 7 : Schematic view of electrostatic levitated motor with additional bias voltage

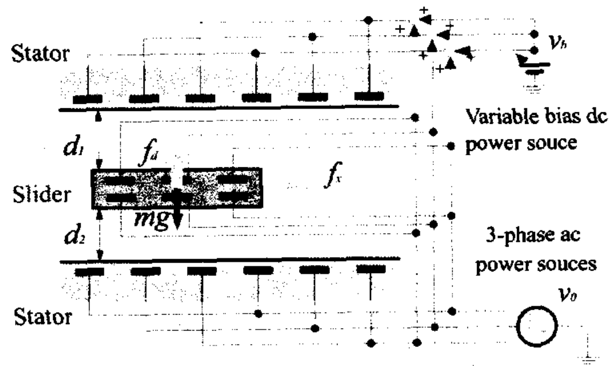

FIGURE 8: Schematic view of electrostatic levitated motor with two opposed sets

addition to that, by using v_b effectively, we can control attractive force independently from thrust force control.

Type 2

In steady state of levitated motor, attractive force f_d must be equilibrated with slide mass. Therefore, in type 1, when the system is in steady state, attractive force f_d should satisfy

$$f_d = \frac{3}{4}\left(k_0(d)v_0^2 + k_b(d)v_b^2\right) = mg \tag{19}$$

where, m represents slider mass. From equation (19), the following relationship about v_0 is derived.

$$v_0 \le \sqrt{\frac{4}{3k_0(d)}mg} \tag{20}$$

Therefore, thrust force f_x is limited:

$$f_x \le \frac{2\pi C_a(d)}{pk_0(d)}mg \tag{21}$$

To remove the limitation, utilization of two sets of slider and stator is proposed as type 2. As shown in Figure 8, the two sets are located as opposed to each other. If we control the gap so that $d_1 = d_2 = d$ in steady state, thrust force and attractive force are calculated from equation (17) as:

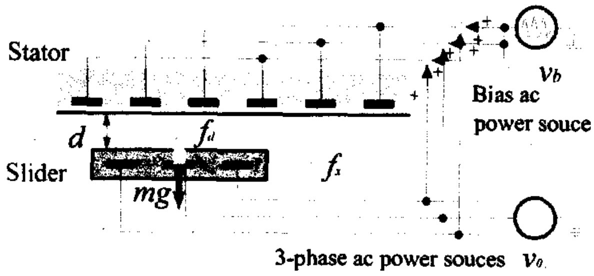

FIGURE 9: Schematic diagram of electrostatic levitated motor with superposed ac voltage

$$\begin{cases} f_x = \dfrac{3\pi C_a(d)}{p} v_0^2 \\ f_d = \dfrac{3}{2} k_b(d) v_b^2 \end{cases} \quad (22)$$

In type 2, thrust force and attractive force are independently controlled by v_0 and v_b.

Type 3

Type 1 and 2 utilizes dc bias voltage to control attractive force. However, continuous applying of dc bias voltage may cause electrostatic charges, which affect motor performances, on films of DEMED. Besides, superposing dc bias high-voltage onto driving high-voltages is not an easy task.

To solve these problems, utilization of ac bias voltage is proposed as type 3. By using ac bias, we can prevent charging of films. In addition to that, ac bias voltage can be easily superposed by using transformers. Figure 9 shows a schematic diagram of type 3. In type 3, voltage vector $\boldsymbol{v}$ is given as $[v_0\sin(\phi),\ v_0\sin(\phi-2\pi/3),\ v_0\sin(\phi+2\pi/3),\ v_0\sin(\phi)+v_b\sin(\omega t),\ v_0\sin(\phi+2\pi/3)+v_b\sin(\omega t),\ v_0\sin(\phi-2\pi/3)+v_b\sin(\omega t)]$. From equation (2) and (8), thrust force and attractive force of type 3 are calculated as:

$$\begin{cases} f_x = \dfrac{3\pi C_a(d)}{2p} v_0^2 \\ f_d = \dfrac{3}{4}\left(k_0(d) v_0^2 + \dfrac{1}{2} k_b(d)(1-\cos(2\omega t)) v_s^2 \right) \end{cases} \quad (23)$$

According to equation (23), f_d fluctuates with an angle frequency of 2ω. However, if this frequency is higher enough than mechanical response frequency, attractive force f_d in equation (23) can be approximated by averaging one period of fluctuation as:

$$\overline{f_d} = \frac{3}{4}\left(k_0(d) v_0^2 + \frac{1}{2} k_b(d) v_s^2 \right) \quad (25)$$

This means ac bias voltage functions as same as dc bias.

CONCLUSION

In this paper, non-contact levitation control system for electrostatic motor was discussed.

Firstly, a relationship between gap and performance of *Dual Excitation Multiphase Electrostatic Drive* (DEMED) was indicated. Elements of DEMED's capacitance coefficients are measured. Thrust force and attractive force of DEMED are calculated theoretically from capacitance coefficients as a function of gap d. Secondly, using bias voltage for controlling attractive force is proposed. Finally, three types of electrostatic levitated motor were proposed and discussed.

ACKNOWLEDGEMENT

This research was supported by a Grant-in-Aid for Scientific Research from Japan Society for Promotion of Science. (Grant No. 12355011)

REFERENCES

1. T. Niino, T. Higuchi, and S. Egawa: "Dual Excitation Multiphase Electrostatic Drive", Conf. Record of 1995 IEEE IAS annual meeting, pp. 1318-1325 (1995)
2. T. Niino, S. Egawa, and T. Higuchi: "High-power and High-efficiency Electrostatic Actuator", Proc. 1993 IEEE Workshop on Micro Electro Mechanical Systems, pp. 236-241 (1993)
3. A. Yamomoto, T. Niino, and T. Higuchi: "A High-Power Electrostatic Linear Servo Motor", Proc. LDIA '98, pp. 212-215 (1998)
4. H. W. Knoebel: "The Electric Vacuum Gyro", Control Engineering, Vol.11, p70, (1964)
5. S. Kumar, D. Cho, W. Carr: "A Proposal for Electrically Levitating Micromotors", Sensors and Actuators A, Vol.24, p141, (1990)
6. J. U. Joen, T. Higuchi: "Induction Motors with Electrostatic Suspension", Journal of Electrostatics,Vol.45, p157, (1998)
7. A. Yamamoto, T. Niino, and T. Higuchi: "High Power Electrostatic Actuator with Novel Electrode Design", Proc. IEEE MEMS '98, pp408-413 (1998)
8. A. Yamamoto, T. Niino, and T. Higuchi: "Servo Control of High-Power Electrostatic Linear Motor", Proc. of the ICMT '99, pp274-279 (1999)